

Blue laser cooling transitions in Tm I

N. Kolachevsky, A. Akimov, I. Tolstikhina, K. Chebakov,
A. Sokolov, P. Rodionov, S. Kanorski, V. Sorokin

P.N. Lebedev Physics Institute, Leninsky prospekt 53, 119991 Moscow, Russian Federation

E-mail: kolik@lebedev.ru, Fax: +7 495 1326644

Pacs: 32.70.Cs, 32.10.Fn, 32.80.Pj

Received: date / Revised version: date

Abstract We have studied possible candidates for laser cooling transitions in ^{169}Tm in the spectral region 410–420 nm. By means of saturation absorption spectroscopy we have measured the hyperfine structure and rates of two nearly closed cycling transitions from the ground state $4f^{13}6s^2(^2F_0)(J_g = 7/2)$ to upper states $4f^{12}(^3H_5)5d_{3/2}6s^2(J_e = 9/2)$ at 410.6 nm and $4f^{12}(^3F_4)5d_{5/2}6s^2(J_e = 9/2)$ at 420.4 nm and evaluated the life times of the excited levels as 15.9(8) ns and 48(6) ns respectively. Decay rates from these levels to neighboring opposite-parity levels are evaluated by means of Hartree-Fock calculations. We conclude, that the strong transition at 410.6 nm has an optical leak rate of less than $2 \cdot 10^{-5}$ and can be used for efficient laser cooling of ^{169}Tm from a thermal atomic beam. The hyperfine structure of two other even-parity levels which can be excited from the ground state at 409.5 nm and 418.9 nm is also measured by the same technique. In addition we give a calculated value of $7(2)\text{s}^{-1}$ for the rate of magnetic-dipole transition at $1.14\text{ }\mu\text{m}$ between the fine structure levels $(J_g = 7/2) \leftrightarrow (J'_g = 5/2)$ of the ground state which can be considered as a candidate for applications in atomic clocks.

1 Introduction

During the last decade, significant progress has been achieved in laser cooling of lanthanides (rare-earth elements). Laser-cooled lanthanides are effectively used in such fundamental fields as the study of cold collisions [1], Bose-Einstein condensation [2], ultra-precise atomic clocks [3] and also open new perspectives for implementation in nano-technology [4] and quantum information [5]. In contrast to recently demonstrated method of buffer gas cooling and trapping of lanthanides in a magnetic dipole trap [6], laser-

cooled atoms are easily manipulated by the help of light fields [7] and can be studied in a nearly perturbation-free regime.

Compared to atoms from the alkali and the alkali-earth groups, spectra of lanthanides are significantly richer due to the presence of the 4f shell electrons. Ytterbium with its closed $4f^{14}$ shell possesses the simplest level structure and has been successfully laser cooled at the wavelength of 398.9 nm (see e.g. [8]). In 2006 cooling of atomic erbium was reported [9] at the wavelength of 401 nm. Both these strong cooling transitions are not completely closed and their upper levels also decay to the neighboring opposite-parity levels thus taking a part of population out from the cooling cycle (optical leaks). In the case of erbium ($4f^{12}6s^2$), evaluation of a leak rate is a complex task due to a rich level structure. Still, it has been shown experimentally, that it is possible to cool and to trap up to 10^6 erbium atoms in a magneto-optical trap (MOT) even without a repumper laser.

In this paper, we analyze the possibility to cool atomic thulium which resides between Er and Yb in the periodic table. Since there is only one unfilled electron in the 4f shell (the ground state of Tm has a configuration of $4f^{13}6s^2(^2F_0)$), its electronic structure is more complex than that of Yb, but still is one of the simplest among lanthanides. Thulium has only one stable isotope ^{169}Tm with a nuclear spin number of $I = 1/2$ which results in a simple doublet hyperfine splitting of each electronic level. The monoisotopic structure should increase a MOT loading rate, while the non-degenerate Zeeman structure of the ground level enables sub-Doppler cooling schemes.

The ground state of ^{169}Tm consists of two fine structure levels with total electronic momentum numbers of $J_g = 7/2$ and $J'_g = 5/2$ which are separated by $2.6 \cdot 10^{14}$ Hz (the corresponding transition wavelength is $\lambda = 1.14 \mu\text{m}$). The excited ground-state level with $J'_g = 5/2$ is metastable and one can expect its life time to be on the order of a few fractions of a second [10]. Due to the shielding by the outer closed $6s^2$ shell [6,11], it is expected that interrogation of these forbidden transitions even in dense laser-cooled atomic clouds will allow one to build precise optical atomic references possessing a high short-term stability.

In this paper we describe our experimental study of two candidates for cooling transitions from the ground state to the excited states $4f^{12}(^3H_5)5d_{3/2}6s^2(J_e = 9/2)$ at 410.6 nm and $4f^{12}(^3F_4)5d_{5/2}6s^2(J_e = 9/2)$ at 420.4 nm (Section II). The hyperfine structure (HFS) of these levels are accurately determined from the experiment. Simultaneously we have for the first time determined the HFS of two other excited levels which are within reach of our laser system. From the analysis of saturation absorption spectra we have experimentally determined lifetimes of the excited levels and compared them with existing data [12]. With the relativistic Hartree-Fock code of Cowan [13], optical leak rates are quantitative evaluated. Results of this analysis are presented in Section III. In Section IV we discuss realistic laser cooling schemes for thulium. In the last Section we analyze the magnetic dipole transition at $1.14 \mu\text{m}$ with the help of the Cowan code and also with the flexible atomic code (FAC) of Feng [14].

2 Saturation absorption spectroscopy

To efficiently laser cool an atomic sample one has to choose a strong closed cycling transition which can be excited by a powerful laser source. In the case of thulium, we restrict our consideration to transitions from the ground state level $4f^{12}6s^2(J_g = 7/2)$ to the excited levels of the opposite parity with $J_e = 9/2$. Such a choice allows the use of cycling transitions between the hyperfine components of the lower and upper levels $F_g = 4 \leftrightarrow F_e = 5$. In this case, electric dipole transitions from upper levels to other fine and hyperfine sublevels of the ground state will be forbidden by the selection rules.

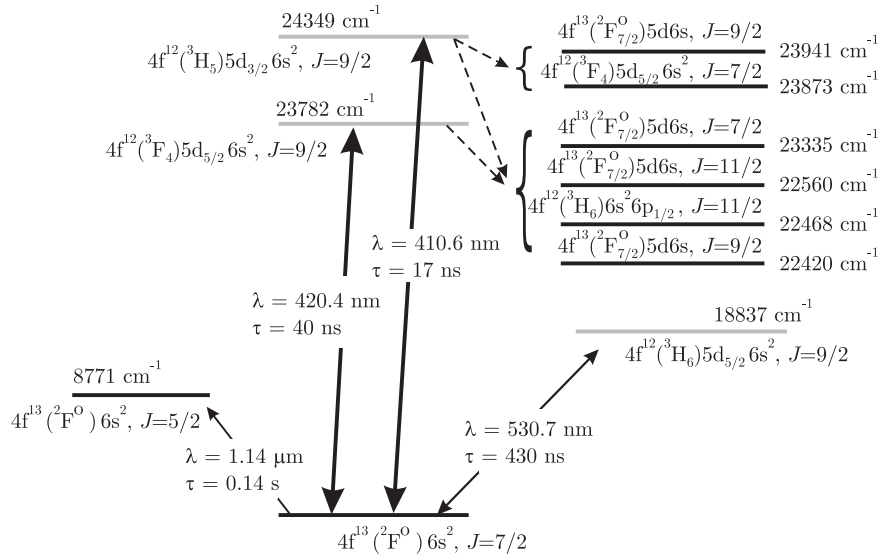


Fig. 1 A partial level diagram of atomic thulium. Even and odd levels are shown in gray and black respectively. Some transition wavelengths and the life times of the corresponding excited levels are presented.

Among excited levels in Tm one can select three candidates favorable for laser cooling [15]: $4f^{12}(^3H_6)5d_{5/2}6s^2$ ($E = 18837 \text{ cm}^{-1}$), $4f^{12}(^3F_4)5d_{5/2}6s^2$ ($E = 23782 \text{ cm}^{-1}$) and $4f^{12}(^3H_5)5d_{3/2}6s^2$ ($E = 24349 \text{ cm}^{-1}$), which are schematically presented in Fig. 1. The green transition at $\lambda = 530.7 \text{ nm}$ can be excited by the second harmonic of a laser on gadolinium scandium gallium garnet activated by neodymium (Nd:GSGG) [16]. The transition is completely closed in the electric-dipole approximation which removes the problem of optical leaks. Unfortunately, the low rate of $A = 2.3 \cdot 10^6 \text{ s}^{-1}$ prevents using this transition for efficient loading a MOT from a thermal beam (an atom with initial velocity of 200 m/s can be decelerated at a distance not shorter than 3 m). Nevertheless it can be used after cooling an atomic

sample at other strong transition. For example, such a blue and green MOT sequence is implemented for cooling ytterbium to sub-mK temperatures [8].

Other transitions at 420.4 nm and 410.6 nm can be excited by the second harmonic of a titanium:sapphire (Ti:Sa) laser, the second harmonic of an infrared diode laser or directly by a nitride diode laser (see e.g. [17]). According to [12] these transitions have rates of $2.43 \cdot 10^7 \text{ s}^{-1}$ and $6.36 \cdot 10^7 \text{ s}^{-1}$ respectively which should be sufficient to decelerate hot atoms at a distance of a few tens of centimeters. The transitions are not completely closed. The upper levels are coupled to neighboring opposite-parity levels as shown in Fig.1. To choose the best candidate for cooling transition it would be desirable to evaluate optical leak rates.

The hyperfine structure of excited levels in thulium is measured by different methods and the following references summarize most of the available data [18,19,20,21,22]. The level with the energy $E = 24\,349 \text{ cm}^{-1}$ has been previously studied by the optogalvanic spectroscopy in the hollow cathode discharge [21] and its HFS frequency has been determined. We use saturation absorption spectroscopy in counter-propagating beams of the same frequency to measure the HFS of the levels which can be excited from the ground state in the wavelength region 410 – 420 nm. The experimental setup is presented in Fig. 2.

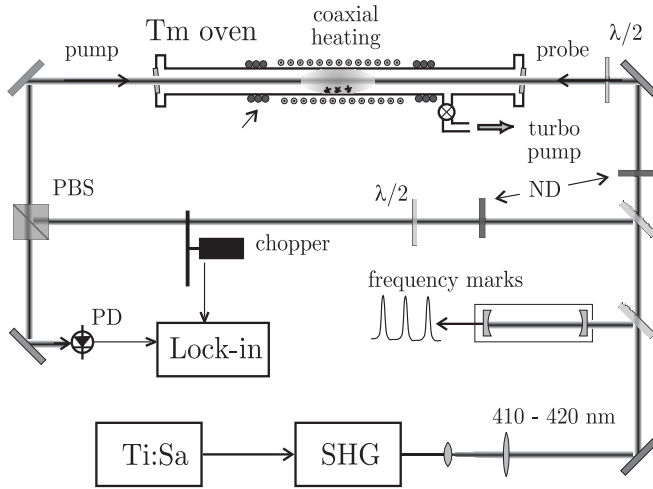


Fig. 2 Saturation absorption spectroscopy setup with lin⊥lin polarizations. Thulium is heated in a stainless steel vacuum cell to 1000 K by a coaxial heating cable. A stable interferometer is used to calibrate recorded spectra. Here SHG is a second harmonic generation stage, PBS – a polarization beam splitter, PD – a silicon photodetector, and ND – variable neutral density filters.

Radiation of a Ti:Sa laser (MBR-110, Coherent Inc.) is frequency doubled in a lithium triobate crystal (LBO) placed in an external cavity (MBD-200, Coherent Inc.). The laser system produces up to 150 mW of radiation in

the spectral region 400–430 nm. The spectral line width of the Ti:Sa laser is specified as 100 kHz which is achieved by locking the laser to a stable high-finesse Fabry-Perot cavity. We tune the laser to the atomic transition with the help of a home-made wavemeter. The astigmatic blue laser beam is expanded to about $w_{0,x} \times w_{0,y} \approx 3 \text{ mm} \times 6 \text{ mm}$ (at $1/e^2$ level) and is split into saturation and probe beams. The beams are carefully aligned in the counter-propagating configuration with the angle between them less than $5 \cdot 10^{-4}$. The probe beam is modulated by a wheel chopper at 850 Hz, and the signal from the probe beam is recorded using the lock-in technique by a computer. The beams have orthogonal linear polarizations ($\text{lin} \perp \text{lin}$) and are separated on a polarization beam splitter. Intensities of the beams can be varied by absorptive neutral density filters. They are measured by a calibrated power meter at the cell entrance. The laser frequency detuning is controlled by a stable confocal interferometer with a free spectral range of 75 MHz. Frequency marks are recorded simultaneously with absorption spectra.

Thulium vapor is produced in a stainless steel oven of 20 mm in diameter. The central part can be heated by a coaxial cable to 1100 K. Current flowing through the central heating wire of the cable returns back through its outer shielding which significantly cancels out an induced magnetic field. External coils in Helmholtz configuration allow compensation of the laboratory magnetic field to less than 1 G. The melting point of thulium is 1818 K, but a vapor pressure of 10^{-3} mbar can be reached already at about 1000 K. To prevent heating of the whole cell, its central part is surrounded by water cooling coils. The cell is pumped out by 20 l/s turbo-molecular pump. Thulium chunks of a few hundred milligrams are placed in the central part of the oven. After heating to 1000 K, we observe the absorption of 50% in the center of the Doppler-broadened line at 410.6 nm. The pipe can stably operate in this regime for days.

Figure 3 presents saturation absorption spectra for the transitions at 410.6 nm and 420.4 nm. Besides saturation absorption lines formed by atoms with zero velocity projection on the beam axis, we observe cross-over resonances of different signs. Identification of hyperfine spectra is presented in the insets of Fig. 2. The accurate result of $-1496.550(1)$ MHz for the HFS of the ground state $4f^{12}6s^2$ ($J_g = 7/2$) measured by Childs *et al.* [18] is used to calibrate the free spectral range of the Fabry-Perot cavity. Here we will use negative frequencies for the HFS if the Fermi energy is negative.

To determine the hyperfine structure frequency of the excited levels we fit the recorded spectra by a multi-peak Lorentzian function and use the frequency ruler of the Fabry-Perot cavity. Uncertainty of the measurement is the sum of the statistical uncertainty of 0.5 MHz and the systematic contribution of 0.5 MHz. The latter mainly results from the asymmetry of transmission peaks of the Fabry-Perot cavity and is evaluated by measuring positions of the cross-over resonances. No dependence of the HFS frequencies on light intensity is observed. Results of the measurement are presented in table 1.

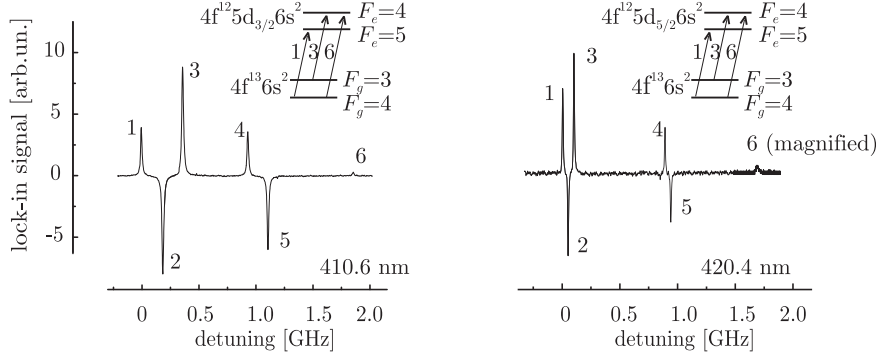


Fig. 3 Saturation absorption spectra of the transitions in ^{169}Tm from the ground state $4f^{13}6s^2(^2F_0)(J_g = 7/2)$ to upper states $4f^{12}(^3H_5)5d_{3/2}6s^2(J_e = 9/2)$ at 410.6 nm and $4f^{12}(^3F_4)5d_{5/2}6s^2(J_e = 9/2)$ at 420.4 nm recorded in lin⊥lin polarizations. Along with saturation absorption resonances, cross-over resonances are observed.

It is interesting to note that the hyperfine splitting of upper and lower levels of both candidates for cooling transitions are similar and differ for only a few tens of natural line widths. It can result in the situation, that a laser tuned to the red wing of the the cooling transition 1 (Fig. 3) will simultaneously transfer population from $F_g = 3$ via the transition 3. Due to the relatively small detuning, the process will have a higher probability than the non-resonance population transfer to the $F_g = 3$ level via $F_e = 4$ one. Laser cooling without repumping has been successfully demonstrated in erbium [9].

The cooling transition rate is a crucial parameter which defines the maximal achievable deceleration of atom as well as the Doppler cooling limit [23]. We use the setup shown in Fig. 2 to measure the natural line width of candidates for cooling transitions $F_g = 4 \leftrightarrow F_e = 5$ at 410.6 nm and 420.4 nm (see insets in Fig. 3). Being excited at these nearly closed cycling

Table 1 The hyperfine splitting frequencies of four excited levels in atomic thulium. The ground state HFS is also given for the reference.

Energy, cm^{-1}	Level	J	HFS splitting, MHz	Reference
0	$4f^{13}6s^2(^2F_0)$	$7/2$	$-1496.550(1)$	[18]
23 781.698	$4f^{12}(^3F_4)5d_{5/2}6s^2$	$9/2$	$-1586.6(8)$	this work
23 873.207	$4f^{12}(^3F_4)5d_{5/2}6s^2$	$7/2$	$+1411.0(7)$	this work
24 348.692	$4f^{12}(^3H_5)5d_{3/2}6s^2$	$9/2$	$-1856.5(2.5)$	[21]
			$-1857.5(8)$	this work
24 418.018	$4f^{13}(^2F_{7/2}^\circ)6s6p(^1P_1^\circ)$	$5/2$	$-1969.4(1.3)$	this work

transitions, thulium behaves as a two-level system which allows us to neglect optical pumping and coherent effects [24].

We performed a set of measurements varying saturation and probe power densities. The power of 1 mW approximately corresponds to the on-axis power density of about 3 mW/cm². Results are presented in Fig. 4, where the measured line width γ is plotted against the excitation power P . Again, each recorded spectrum has been fitted by a multi-peak Lorentzian function with independent fit parameters for each peak. In the case of a weak probe beam, the line width γ is given by the following expression [25, 26]

$$\gamma(I) = \frac{1}{2}\gamma_0(1 + \sqrt{1 + I/I_{\text{sat}}}), \quad (1)$$

where γ_0 is the natural line width and I is an excitation power density. The saturation power density I_{sat} is defined as $I_{\text{sat}} = 2\pi\hbar c\gamma_0/3\lambda^3$. In the general case the expression is more complex [24], but the relation $\gamma(0) = \gamma_0$ remains valid.

We fit the data presented in Fig. 4 by the function (1), where γ_0 and I_{sat} are taken as fit parameters. Due to uncertainty in the power density measurement and inhomogeneous intensity profile we have to use the second fit parameter for I_{sat} . Line widths extrapolated to zero intensity are $\gamma_{410\text{ nm}}(0) = 10.5(2)$ MHz for the transition $F_g = 4 \leftrightarrow F_e = 5$ at 410.6 nm and $\gamma_{420\text{ nm}}(0) = 3.8(1)$ MHz for the corresponding hyperfine transition at 420.4 nm. The inhomogeneous radial intensity distribution should modify the fit function in a complex way. But substitution of the fit function (1) by a linear regression or by a function $\gamma(I) = \gamma_0\sqrt{1 + I/I_{\text{sat}}}$ changes extrapolated values for less than 0.2 MHz. We use this value as an uncertainty resulting from our unprecise knowledge of the fit function. Derivation of true saturation intensity and γ_0 from the second fit parameter is hindered by the complex radial intensity distribution in the laser beams.

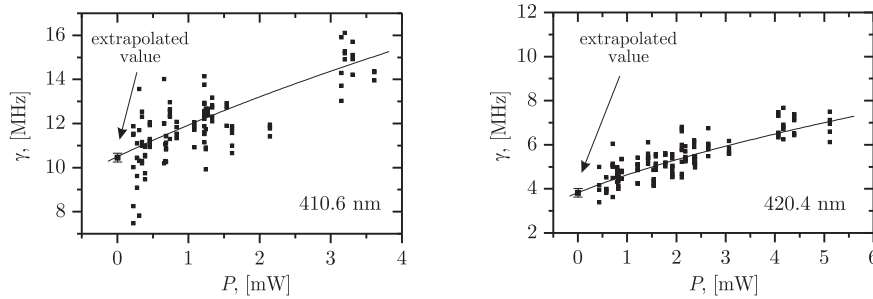


Fig. 4 Spectral line widths γ of the transitions $4f^{13}6s^2(^2F_0)(F = 4) \leftrightarrow 4f^{12}(^3H_5)5d_{3/2}6s^2(F = 5)$ (left, 410.6 nm) and $4f^{13}6s^2(^2F_0)(F = 4) \leftrightarrow 4f^{12}(^3F_4)5d_{5/2}6s^2(F = 5)$ (right, 420.4 nm) versus the excitation power P .

To evaluate the natural line widths of the transitions we correct the obtained results for systematic broadenings. The main contribution results

from the laser line width which we evaluate as 0.2(2)MHz according to the manufacturers specification (we doubled the line width of the Ti:Sa laser assuming that the main noise contribution results from slow long-term correlated acoustic vibrations [27]). The next important broadening mechanism is the time-of-flight broadening which we evaluate as 0.1(1) MHz. The geometrical broadening resulting from the finite angle between the beams and pressure shift can be conservatively estimated as 10(10) kHz and 50(50) kHz respectively. The Zeeman splitting of π -components in a residual magnetic field is small due to very similar magnetic g -factors of the lower and the upper levels. The splitting of σ -components is about 1.5 MHz/G. For magnetic fields lower than 1 G the Zeeman splittings Δ_Z is relatively small ($\Delta_Z \ll \gamma_0$) and can be considered similar to inhomogeneous spectral line broadening. The following expression for the resulting line profile γ_{tot} is valid $\gamma_{\text{tot}} \simeq \sqrt{\gamma_0^2 + \Delta_Z^2}$ which is similar to the case of Voigt function, when the contribution of the Doppler width is much less than of the Lorentzian one. Thus the Zeeman broadening of the transitions can be evaluated as 0.1(2) MHz. Taking all these contributions into account we finally get the natural line width of 10.0(4) MHz for the transition $4f^{13}6s^2(^2F_0)(F=4) \leftrightarrow 4f^{12}(^3H_5)5d_{3/2}6s^2(F=5)$ at 410.6 nm and 3.3(4) MHz for the transition $4f^{13}6s^2(^2F_0)(F=4) \leftrightarrow 4f^{12}(^3F_4)5d_{5/2}6s^2(F=5)$ at 420.4 nm. Our results are in a good agreement with transition rates given in [12, 15] and are summarized in the next Section in table 2.

3 Optical leaks

The candidates for cooling transitions at $\lambda = 410.6$ nm and $\lambda = 420.4$ nm are not perfectly closed. The excited levels $4f^{12}(^3H_5)5d_{3/2}6s^2(J=9/2)$ and $4f^{12}(^3F_4)5d_{5/2}6s^2(J=9/2)$ can decay via electric dipole transitions to 6 and 4 neighboring opposite-parity levels respectively as shown in Fig. 1. A crucial parameter for a cooling transition is a branching ratio

$$k = \frac{\sum A_i}{A_1 + \sum A_i}, \quad (2)$$

where A_1 is the decay rate to the ground state and A_i ($i = 2, \dots, 5$ for the 420.4 nm transition or $i = 2, \dots, 7$ for 410.6 nm one) are decay rates via other dipole transitions. In the expression (2) only the decay rate to the ground state can be taken from [12, 15] while all other values remain unknown.

We evaluated the decay rates using the relativistic Hartree-Fock code of Cowan [13]. The excited states have mixed electronic configurations (see [15]), and we took into account a few leading configurations for each level. Since it is difficult to achieve correct energies for all levels simultaneously, we performed two sets of calculations. In the first set, the experimental energy of $4f^{12}(^3H_5)5d_{3/2}6s^2(J=9/2)$ level ($E = 24\,349 \text{ cm}^{-1}$) was taken as a

reference for calculations after which the required decay rates were calculated. Similar evaluations were made for the $4f^{12}(^3F_4)5d_{5/2}6s^2 (J = 9/2)$ level ($E = 23\,782\text{ cm}^{-1}$). Results of calculations are summarized in table 2.

Table 2 Decay rates of two excited levels $4f^{12}(^3H_5)5d_{3/2}6s^2 (E = 24\,349\text{ cm}^{-1})$ and $4f^{12}(^3F_4)5d_{5/2}6s^2 (E = 23\,782\text{ cm}^{-1})$ in atomic thulium. Energies $E_{g,e}^{\text{COWAN}}$ and corresponding electric dipole transition rates A^{COWAN} are calculated using relativistic code of Cowan [13]. For comparison, we give the energies $E_{g,e}^{\text{W}}$ and rates A^{W} measured in [12] and experimental results of this work A (the right column).

$E_g^{\text{COWAN}},$ 10^3 cm^{-1}	$E_g^{\text{W}},$ 10^3 cm^{-1}	J_g	$E_e^{\text{COWAN}},$ 10^3 cm^{-1}	$E_e^{\text{W}},$ 10^3 cm^{-1}	J_e	$A^{\text{COWAN}},$ s^{-1}	$A^{\text{W}},$ s^{-1}	A (this work), s^{-1}
0.000	0.000	3.5	24.341	24.349	4.5	$2.13 \cdot 10^8$	$6.36(30) \cdot 10^7$	$6.3(3) \cdot 10^7$
22.166	22.420	4.5	24.341	24.349	4.5	$4.44 \cdot 10^2$		
22.243	22.468	5.5	24.341	24.349	4.5	$1.75 \cdot 10^2$		
22.417	22.560	5.5	24.341	24.349	4.5	$1.82 \cdot 10^2$		
22.905	23.335	3.5	24.341	24.349	4.5	$1.38 \cdot 10^2$		
23.622	23.941	4.5	24.341	24.349	4.5	$1.54 \cdot 10^1$		
23.893	23.873	3.5	24.341	24.349	4.5	$2.95 \cdot 10^0$		
0.000	0.000	3.5	23.797	23.782	4.5	$2.27 \cdot 10^7$	$2.43(12) \cdot 10^7$	$2.1(3) \cdot 10^7$
22.166	22.420	4.5	23.797	23.782	4.5	$1.88 \cdot 10^1$		
22.243	22.468	5.5	23.797	23.782	4.5	$1.81 \cdot 10^2$		
22.417	22.560	5.5	23.797	23.782	4.5	$8.64 \cdot 10^2$		
22.905	23.335	3.5	23.797	23.782	4.5	$1.13 \cdot 10^0$		

Calculated energies are in a good agreement with experimental data. Comparing calculated rates of strong transitions to the ground state with ones from [12,15] we observe a significant discrepancy for the transition at 410.6 nm (the first row in table 2). We will take it as a scale for the accuracy of our evaluation. Note, that the transition $4f^{12}(^3F_4)5d_{5/2}6s^2 (J = 9/2) \rightarrow 4f^{13}(^2F_{7/2})5d6s (J = 11/2)$ demonstrates the exceptionally high rate of about 10^3 s^{-1} .

Using the results of table 2 we evaluate the branching ratios according to equation (2):

$$k_{410\text{ nm}} = 1_{-0.5}^{+1} \cdot 10^{-5}, \quad (3)$$

$$k_{420\text{ nm}} = 5_{-2.5}^{+5} \cdot 10^{-5}, \quad (4)$$

where the uncertainties are evaluated according to the discrepancy between calculated and experimental values. To get these values we take experimental rates for A_1 , while other rates A_i are taken from calculations. The given uncertainty is a realistic estimation for the accuracy of our calculations. It would be necessary to mention that not all of the atoms which have decayed

from the excited odd levels to the neighboring even levels are taken away from a laser cooling cycle. Part of them can return back to the ground state by cascade transitions while another part sticks in metastable levels. Calculations of cascaded transitions are a complex task, and it is reasonable to use the approach given in the paper [9], where these excited levels are considered as a “reservoir” slowly feeding the ground state. We use evaluations (3), (4) as upper limits for the optical leak rates.

4 Cooling transition

We have analyzed the possibility to cool atomic thulium from the thermal beam at a temperature of 1100 K using blue resonance light in a Zeeman cooler. Because of the relatively low transition rate and the significant rate of optical leaks, the transition at 420.4 nm looks unfavorable for laser cooling. Indeed, to completely decelerate a thulium atom with the initial velocity of 200 m/s it is necessary to have about 35 000 scattering events. For the transition at 420.4 nm 97% of atoms will be lost during deceleration if we take $k_{420\text{ nm}} = 10^{-4}$ (4). On the other hand, transition at 410.6 nm is more suitable for cooling: for the worst case estimation only 50% of the atoms will be lost. We have numerically modelled the Zeeman slower of 40 cm long [28] and derived, that about 7% of initial number of atoms from the thermal beam can be decelerated to velocities of 20 m/s with all optical leaks (table 2) taken into account. We expect that using the transition at 410.6 nm one can cool and trap in a MOT up to 10^6 thulium atoms with a loading rate of about 1 s for realistic oven and MOT parameters. The repumping field, if necessary, can be produced from the cooling field using an acousto-optical modulator operating at about 360 MHz (see table 1).

The Doppler limit of this transition $T_{\text{dop}} = \hbar A / 2k_B$ (here k_B is the Boltzman constant) corresponds to $230\text{ }\mu\text{K}$ which is too high for successive loading in an optical dipole trap or for making experiments in a ballistic flight. Further cooling can be achieved by e.g. Sisyphus cooling or switching to a green MOT at 530.7 nm with $T_{\text{dop}} = 9\text{ }\mu\text{K}$.

5 Clock transition

As indicated in the Introduction, the transition between the fine-structure levels of the ground state $(J_g = 7/2) \rightarrow (J'_g = 5/2)$ at $1.14\text{ }\mu\text{m}$ can be considered as a candidate for a clock transition due to its low sensitivity to collisions and low differential polarizability of the two states. In the work of Aleksandrov *et al.* [11] this transition has been observed in the absorption spectrum of thulium vapors using a high-resolution spectrometer. Even after adding up to 50 bar of helium to a thulium cell, the authors could not detect any spectral broadening of this transition. They have concluded, that the pressure broadening is less than 20 MHz/bar which is 500 times less than typical broadening of resonance s-p or f-d transitions ($\sim 10\text{ GHz/bar}$).

Using the Cowan code we have evaluated the transition rate at $1.14\ \mu\text{m}$. The magnetic-dipole transition has a rate of $A = 5.9\ \text{s}^{-1}$ while the electric quadrupole transition rate is negligible. The same evaluation has been done with the help of the Flexinle Atomic Code of Gu Ming Feng [14] which results in $A = 7.7\ \text{s}^{-1}$. The results agree with each other and we give the final estimation of $A = 7(2)\ \text{s}^{-1}$ for this transition rate which corresponds to the spectral line width of $1.1(3)\ \text{Hz}$ and the transition Q -factor of $2.4(7) \cdot 10^{14}$. Detection of the narrow unperturbed resonance in a cold atomic cloud produced in MOT should increase the signal to noise ratio and stability of a frequency reference [7]. The transition can be excited by a frequency stabilized ytterbium fiber laser (see e.g. [29] and references therein) or, probably, by a stabilized chromium:forsterite laser ($\text{Cr:Mg}_2\text{SiO}_4$) [30].

6 Conclusions

In this work we have analyzed the possibility to cool atomic thulium using strong blue transitions in the spectral range $410\text{--}420\ \text{nm}$. The hyperfine structure of two candidates for cooling transitions at $410.6\ \text{nm}$ and $420.4\ \text{nm}$ and of two other transitions at $409.5\ \text{nm}$ and $418.9\ \text{nm}$ is determined by means of saturation absorption spectroscopy. From analysis of the spectral line widths we derived the corresponding transition rates with an accuracy better than 10%. We have evaluated the role of optical leaks by calculation of decay rates from the excited levels $4f^{12}(^3\text{H}_5)5d_{3/2}6s^2$ ($E = 24\,349\ \text{cm}^{-1}$) and $4f^{12}(^3\text{F}_4)5d_{5/2}6s^2$ ($E = 23\,782\ \text{cm}^{-1}$) using the code of Cowan [13].

We conclude, that the transition $4f^{13}6s^2(^2\text{F}_0)(F_g = 4) \leftrightarrow 4f^{12}(^3\text{F}_4)5d_{5/2}6s^2(F_e = 5)$ at $410.6\ \text{nm}$ can be used for effective laser cooling of thulium from a hot atomic beam. Evaluations show, that deceleration of atomic beam in a 40-cm Zeeman slower will allow one to decelerate about 5% of atoms from the thermal distribution and to trap up to 10^6 atoms in a magneto-optical trap. Further cooling can be achieved in a green MOT operating at $\lambda = 530.7\ \text{nm}$.

We have evaluated the rate of the electric-dipole forbidden transition at $1.14\ \mu\text{m}$ between the fine structure levels of the ground state $(J_g = 7/2) \rightarrow (J'_g = 5/2)$. A calculated rate of the magnetic-dipole transition is $A = 7(2)\ \text{s}^{-1}$ which corresponds to the quality factor of $2 \cdot 10^{14}$. This shielded transition can be considered as one of the candidates for applications in optical atomic clocks.

Acknowledgments

The work is partly supported by the Alexander von Humboldt Foundation, Russian Science Support Foundation and RFBR Grants #05-02-16801, #08-02-00667, #05-02-00443.

References

1. L. Santos, G.V. Shlyapnikov, P. Zoller, and M. Lewenstein: *Phys. Rev. Lett.* **85**, 1791 (2000)
2. Y. Takasu, K. Maki, K. Komori, T. Takano, K. Honda, M. Kumakura, T. Yabuzaki, Y. Takahashi: *Phys. Rev. Lett.* **91**, 040404 (2003)
3. Z.W. Barber, C.W. Hoyt, C.W. Oates, L. Hollberg, A.V. Taichenachev, and V.I. Yudin: *Phys. Rev. Lett.* **96**, 083002 (2006)
4. S.B. Hill and J.J. McClelland: *Appl. Phys. Lett.* **82**, 3128 (2003)
5. C. Monroe: *Nature* **416**, 238 (2002)
6. C.I. Hancox, S.C. Doret, M.T. Hummon, L. Luo, J.M. Doyle: *Nature* **431**, 281 (2004)
7. H. Katori, M. Takamoto, V.G. Pal'chikov, and V.D. Ovsjannikov: *Phys. Rev. Lett.* **91**, 173005 (2003)
8. R. Maruyama, R.H. Wynar, M.V. Romalis, A. Andalkar, M.D. Swallows, C.E. Pearson, and E.N. Forston: *Phys. Rev. A* **68**, 011403(R) (2003)
9. J.J. McClelland and J.L. Hanssen: *Phys. Rev. Lett.* **96**, 143005 (2006)
10. H.Y. Ban, M. Jacka, J.L. Hanssen, J. Reader, and J.J. McClelland: *Optics Express* **13**, 3185 (2005)
11. E.B. Aleksandrov, V.N. Kotylev, V.N. Kulyasov, and K.P. Vasilevskii: *Opt. Spektrosk.* **54**, 3 (1983).
12. M.E. Wickliffe and J.E. Lawler: *J. Opt. Soc. Am. B* **14**, 737 (1997)
13. R.D. Cowan: *The theory of atomic structure and spectra*, (University of California Press, Berkeley, CA, 1981), and Cowan programs RCN, RCN2, and RCG
14. Gu Ming Feng: *ATOMIC PROCESSES IN PLASMAS: 14th APS Topical Conference on Atomic Processes in Plasmas. AIP Conference Proceedings* **730**, 127 (2004)
15. <http://www.physics.nist.gov/PhysRefData/ASD/index.html>
16. Y.V. Zarikov et. al.: *Kvantovaya Elektronika* **11**, 1565 (1984)
17. J. Hult, I.S. Burns, C.F. Kaminski: *Applied Optics* **44**, 3675 (2005)
18. W.J. Childs, H. Crosswhite, L.S. Goodman, and V. Pfeufer: *J. Opt. Soc. Am. B* **1**, 22 (1984)
19. K.A.H. van Leeuwen, E.R. Eliel and W. Hogervorst: *Physics Letters* **78A**, 54 (1980)
20. V. Pfeufer: *Z. Phys. D – Atoms, Molecules and Clusters* **4**, 351 (1987)
21. S. Kröger, L. Tanriver, H.-D. Kronfeldt, G. Guthöhrlein, H.-O. Behrens: *Z. Phys. D* **41**, 181 (1997)
22. G. Başar, G. Başar, İ.K. Öztürk, F.G. Acar, and S. Kröger: *Physica Scripta* **71**, 159 (2005)
23. J.J. McClelland: *Phys. Rev. A* **73**, 064502 (2006)
24. V.S. Letochov and V.P. Chebotaev: *Nonlinear Laser Spectroscopy*, edited by D.L. McAdam (Springer, Berlin, 1977), Vol. 4
25. P.G. Pappas, M.M. Burns, D.D. Hinshelwood, and M.S. Fels: *Phys. Rev. A* **21**, 1955 (1980)
26. S.I. Ohshima, Y. Nakadan, and Y. Koga: *IEEE Journal of Quantum Electronics* **23**, 473 (1987)
27. S.M. Rytov, Yu.A. Kravtsov, V.I. Tatarski: *Principles of statistical radio-physics* Vol. 2, p. 59, (Springer, Berlin Heidelberg 1988).
28. T.E. Barrett, S.W. Daport-Schwartz, M.D. Ray, and G.P. Lafyatis: *Phys. Rev. Lett.* **67**, 3483 (1991)

29. A.S. Kurkov, V.M. Paramonov, and O.I. Medvedkov: Laser Phys. Lett. **3**, 503 (2006)
30. A. Sennaroglu: Applied Optics **41**, 4356 (2002)